

Near Infra-Red Spectroscopy Predicts Crude Protein in Hemp Grain

Ryan Crawford¹, Jamie Crawford¹, Lawrence B. Smart², Virginia Moore³

¹Cornell University, Ithaca, NY,

²Cornell AgriTech, Geneva, NY,

³Cornell University, Ithaca, NY,

Corresponding author: Ryan Crawford, rvc3@cornell.edu

Abstract

Lorem ipsum dolor sit amet, consectetur adipiscing elit, sed do eiusmod tempor incididunt ut labore et dolore magna aliqua. Ut enim ad minim veniam, quis nostrud exercitation ullamco laboris nisi ut aliquip ex ea commodo consequat. Duis aute irure dolor in reprehenderit in voluptate velit esse cillum dolore eu fugiat nulla pariatur. Excepteur sint occaecat cupidatat non proident, sunt in culpa qui officia deserunt mollit anim id est laborum.

Plain Language Summary

Earthquake data for the island of La Palma from the September 2021 eruption is found ...

incomplete: may contain errors, run-ons, half-thoughts, etc.

0.1 INTRODUCTION

Hemp (*Cannabis sativa* L.) is an annual crop with potential uses as a source of food or feed from grain, and bast fiber or hurd from the stalk. Hemp cultivars are commonly grown for one or both purposes and a cultivar may be referred to as a grain, fiber, or dual-purpose type. Because of protein's nutritional importance, the protein content of a grain crop is an prime consideration for researchers, producers, and consumers. Whole hemp grain typically contains approximately 20-30% protein (Bárta et al., 2024; Callaway, 2004; Ely & Fike, 2022). Crude protein (CP) is often used as a proxy for the direct measurement of protein concentration and consists of the multiplication of nitrogen concentration by a conversion factor because measuring nitrogen concentration is relatively simple (Hayes, 2020).

Near-infrared spectroscopy (NIRS) technology is rapid, non-destructive, and cheap. It consists of the measurement of NIR radiation reflected and absorbed from a sample (the spectra) and the relation of the spectra to laboratory values for components such as moisture, protein, fat, or fiber (Roberts et al., 2004). NIRS technology has been used since the 1970's to assess forage CP (Reeves, 2012; Williams, 1975). A NIRS calibration set often consists of samples from one species grown in many environments encompassing the range of expected values from the analyte or analytes (Chadalavada et al., 2022). Partial least squares regression (PLSR) is a typical method used in the agricultural and food sciences to relate spectra to analyte (Roberts et al., 2004). PLSR calculates components that maximize covariance between predictor and response variables. PLSR uses some number of components, often selected via cross-validation, in order to fit the regression model and is commonly used in spectroscopy because it tends to work well with highly-correlated, noisy spectral data (Wold et al., 2001).

A NIRS-scanned sample of undamaged grain may used for other purposes besides its scan or it may planted as a seed. In wheat and corn, grain protein content has been shown to be heritable (Geyer et al., 2022; Giancaspro et al., 2019). This suggests (at least potentially) that NIRS technology could serve as resource to rapidly identify high CP hemp germplasm, enabling the screening of more germplasm as grain, before planting to the field, and thus enabling the more efficient development of high CP hemp grain cultivars.

For this study, a benchtop NIR spectrometer was used to develop a model to predict CP content based on a data set of hemp grain representing multiple years, locations, and cultivars from grain and dual-purpose hemp types using PLSR.

0.2 MATERIALS AND METHODS

Source: [Article Notebook](#)

Source: [Article Notebook](#)

0.2.1 Hemp Grain Sample Background

Spectral data were obtained from whole (unground) hemp grain samples, harvested at maturity, collected from 2017 - 2021 from 18 cultivar trials in New York (NY) (NA samples). Grain samples were obtained by hand sampling or mechanical harvest and were cleaned of chaff and dried at 30 C for six days in a forced-air dryer. In total, 38 cultivars were represented in the data set. Cultivars were grain or dual-purpose types and included both commercially available and experimental material.

All cultivar trials were planted in randomized complete block design with each cultivar replicated four times. The 2017 data were comprised of samples from the same thirteen cultivars sampled from six NY locations. For those trials, grain was harvested from each plot individually and aggregated by cultivar within each trial. Four subsamples were drawn from each aggregated sample and scanned separately. These spectra were averaged at each 2 nm increment. All remaining samples from 2018-2021 were collected on a per-plot basis. All possible cultivars and possible locations were represented in 2017, but only a selected subset of cultivars and locations were represented in 2018-2021.

0.2.2 Spectral Data Collection and Preprocessing

A benchtop NIR spectrometer (FOSS/ NIR FOSS/ NIR Systems model 5000) was used to obtain the spectra (FOSS North America, Eden Prairie, MN, USA). Spectra were collected every 2 nm from 1100-2498 nm and the logarithm of reciprocal reflectance was recorded. A 1/4 rectangular sample cup (5.7 cm × 4.6 cm) was used.

WINISI software version 1.02A (Infrasoft International, Port Matilda, PA, USA) was used to average the spectra in 2017, as well as to select samples for laboratory assay. Samples were selected according to their spectral distance from their nearest neighbor within the calibration data set with a cutoff of a distance of 0.6 H, where H is approximately equal to the squared Mahalanobis distance divided by the number of principal components used in the calculation (Garrido-Varo et al., 2019). Prior to selection selection, spectra were preprocessed using SNV-detrend with settings 1,4,4,1 for the derivative, gap, smooth, and smooth 2 settings respectively.

0.2.3 Laboratory Validation

Laboratory assays were performed by Dairy One Forage Laboratory (Ithaca, NY). For those assays, 1mm ground samples were analyzed by combustion using a CN628 or CN928 Carbon/Nitrogen Determinator. Samples from 2017 were aggregated as described above, but the remaining samples were not aggregated.

0.2.4 Model Development

Calibration and validations sets were created by dividing the laboratory CP values into tertiles according to their percent CP in order to ensure that the range of CP values was present in both calibration and testing sets. Within each tertile, 75% of the samples were randomly assigned to the calibration set and the remaining 25% were assigned to the testing set. For each calibration set, models were developed in the caret package using PLSR. In fitting the model, the number of components was optimized over a grid search from 1-20. Model performance was evaluated with 25 iterations of bootstrapping and minimized root mean squared error (RMSE) in selecting the number of components in the final model.

Source: [Article Notebook](#)

Initially a number of common spectral preprocessing methods were tested by creating 100 calibration and testing sets, as described above. Spectral data from those data sets were transformed by each of the following methods: 1) first derivative, 2) Savitzky-Golay (SG) using the first derivative, third order polynomial, and a window of size 5, 3) gap-segment derivative using the first derivative, a gap of eleven, and a segment size of 5, 4) standard normal variate (SNV), 5) standard normal variate fol-

lowing Savitzky-Golay (SNV-SG) (same SG parameters as above), 6) SNV-detrend with second order polynomial, and 7) multiplicative scatter correction. For comparison, models were also developed using untransformed spectra.

For each of these preprocessing methods, models were fit and predictions were made on the corresponding validation set (since there were 8 preprocessing methods, 8 separate models were fit for each of the 100 sets. The relationship between the predicted and actual values of the test set were calculated via RMSE, coefficient of determination (R^2), relative predicted deviation (RPD), and Ratio of Performance to InterQuartile distance (RPIQ), four common model assessment metrics. Larger R^2 , RPD and RPIQ values and smaller RMSE values are best. The answer to the question of exactly which values constitute a “good” model varies depending upon the reference consulted, but for simplicity’s sake we searched for a model with $R^2 > 0.80$, an RPD greater than 2.5 and ideally greater than 3 (“good” to “excellent” quantitative prediction), and an RPIQ greater than 2.3 but ideally greater than 4.1. (Chadalavada et al., 2022; Luce et al., 2017; Rawal et al., 2024).

Analyses of variance (ANOVA) were performed for each of these metrics in order to compare the preprocessing methods. For each ANOVA, each data set was considered as a subject and different variances were allowed for each preprocessing method. Once the most promising preprocessing method was identified, 1000 more data sets were created and analyzed via that method and performance on the testing sets was summarized with RMSE, R^2 , RPD, and RPIQ. The pattern of errors, expressed as the difference between the actual and predicted values for a given sample, was examined.

0.2.5 Additional software used

We used R version 4.3.3 (R Core Team, 2024) and the following R packages: caret v. 6.0.94 (Kuhn & Max, 2008), data.table v. 1.15.2 (Barrett et al., 2024), emmeans v. 1.10.0 (Lenth, 2024), nlme v. 3.1.163 (J. Pinheiro et al., 2023; J. C. Pinheiro & Bates, 2000), pls v. 2.8.3 (Liland et al., 2023), prospectr v. 0.2.7 (Stevens & Ramirez-Lopez, 2024), skimr v. 2.1.5 (Waring et al., 2022), tidymodels v. 1.1.1 (Kuhn & Wickham, 2020), tidyverse v. 2.0.0 (Wickham et al., 2019).

Source: [Article Notebook](#)

0.3 RESULTS AND DISCUSSION

0.3.1 Laboratory assay CP values

Laboratory assay percent CP values are summarized in the following table. These are similar to the range of CP values observed in the literature, indicating an reasonable basis for a chemometric model. The CP values are left-skewed and two thirds of the samples contained more than 25% CP.

Table 1: Summary of Laboratory Assayed CP Values (Percent Dry Matter)

Mean	Sd	Minimum	First Quartile	Median	Third Quartile	Maximum
26.1	2.5	20.8	23.9	26.4	28.2	30.8

Source: [Article Notebook](#)

0.3.2 Preprocessing methods comparison

Source: [Article Notebook](#)

Source: [Article Notebook](#)

Source: [Article Notebook](#)

Source: [Article Notebook](#)

Source: [Article Notebook](#)

Source: [Article Notebook](#)

All preprocessing methods outperformed untransformed spectral data Table 2. Averaged together, all preprocessed spectra were superior to untransformed spectra, with lower RMSE, and higher R^2 , RPD and RPIQ values (significant at α level <0.001). Preprocessing methods had -11.6 % lower RMSE, and had 3.1% higher R^2 , 6.3% higher RPD and 7.4% higher RPIQ than unprocessed spectra. Preprocessed spectra also had lower standard errors than untransformed spectra.

The SNV-SG method had the lowest RMSE and the highest R^2 , RPD and RPIQ averaging over all iterations. SNV-SG RMSE averaged 1.4% lower, while R^2 , RPD, and RPIQ averaged 0.4%, 2.1%, and 2.4% higher respectively than the next best preprocessing method (SG in both cases), but the differences between the best and second best methods by metric were only statistically significant at $\alpha < 0.05$ for RPD and RPIQ. There is a long history of using RPD to evaluate chemometric models although the statistic has been criticized as inadequately reflecting the distribution of skewed populations, a situation for which RPIQ was the more modern successor (Bellon-Maurel et al., 2010). Here the data were somewhat but not heavily skewed and RPD and RPIQ metrics were in agreement. The superiority of SNV-SG by these metrics made it the best choice for the final model.

Table 2: Evaluation of Preprocessing Methods by Metric \pm Standard Error

Preprocessing Method	RMSE	R^2	RPD	RPIQ
Standard Normal Variate following	1.02 \pm	0.84 \pm	2.49 \pm	3.97 \pm
Savitzky-Golay	0.012	0.004	0.032	0.076
Savitzky-Golay	1.03 \pm	0.83 \pm	2.44 \pm	3.88 \pm
	0.012	0.004	0.029	0.072
First Derivative	1.07 \pm	0.82 \pm	2.36 \pm	3.77 \pm
	0.013	0.004	0.032	0.075
Standard Normal Variate	1.12 \pm	0.80 \pm	2.26 \pm	3.61 \pm
	0.016	0.005	0.036	0.081
Gap-segment Derivative	1.12 \pm	0.81 \pm	2.26 \pm	3.60 \pm
	0.018	0.006	0.040	0.086
Standard Normal Variate-Detrend	1.13 \pm	0.80 \pm	2.22 \pm	3.55 \pm
	0.015	0.005	0.035	0.079
Multiplicative Scatter Correction	1.17 \pm	0.79 \pm	2.17 \pm	3.47 \pm
	0.016	0.006	0.035	0.080
Untransformed Spectra	1.22 \pm	0.79 \pm	2.17 \pm	3.42 \pm
	0.044	0.009	0.052	0.105

Source: [Article Notebook](#)

These results are not surprising. SNV and SNV-detrend both correct light scatter, which is often a function of differences in particle size and sample packing density, although SNV-detrend is often used for densely-packed, powdered samples (Barnes et al., 1989). SG is a smoothing filter that regresses on the signal over a series of windows, removing noise while preserving the signal’s shape and features (Li et al., 2020; Luo et al., 2005). Derivatives, here including SG, gap-segment, and first derivatives pretreatments may remove additive and multiplicative effects, but not necessarily light scatter; as well, derivatives may increase spectral noise (Rinnan et al., 2009). Here, hemp grain was neither powdered nor densely packed but samples were subject to light scatter and noise due to differences in particle size in the grain.

The preprocessing methods examined represent a portion of those available. As well, these methods tend to have a number of user-adjustable parameters whose various permutations were not tested. This subset of preprocessing methods and parameters nonetheless contained substantial variations in model quality, demonstrating the importance of selecting an appropriate preprocessing method.

0.3.3 Final model development and summary

Source: [Article Notebook](#)

The model improved most rapidly as the number of components increased from 1 to 7, with the inclusion of each additional component being associated with a decrease in RMSE of 5-12%. From 8 to 12 components, model performance continued to improve, although gains were more modest (there was a decrease in RMSE of 0.7-3% with the inclusion of each additional component). With 13 or more components, performance gains were minimal and the relative ranks of the models tended to be stable Figure 1.

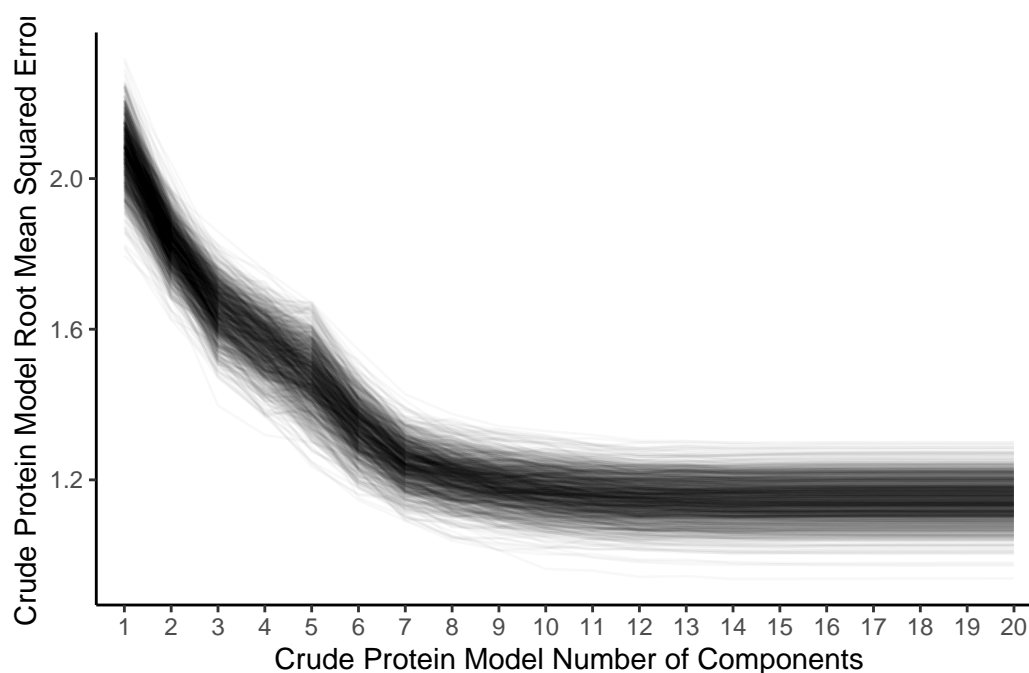


Figure 1: Decreasing RMSE with increasing number of PCs

Source: [Article Notebook](#)

Source: [Article Notebook](#)

Source: [Article Notebook](#)

Final models performances on the test sets were similar, but not identical to, that obtained during the initial comparison of preprocessing methods. The final models' mean RMSE was 1.03, R^2 was 0.83, RPD was 2.44, and RPIQ was 3.89. Five percent of the models were excellent by both metrics, with RPD > 3 and RPIQ > 4.1 , while an additional 11% of the models were "good" by both metrics (RPD range from 2.5 - 3.0, RPIQ range from 2.3 - 4.1). Forty-nine percent of the models had the ability to approximate quantitative prediction (RPD range from 2.0 - 2.5), and 9% of the models were able to distinguish between higher and lower CP values (RPD

range from 1.5 - 2.0). Therefore, 74% of the models generated here had, at minimum, the ability to distinguish between high and low values with with two thirds of them having, at minimum, the ability to approximate quantitative prediction. Despite the generally good model performance, a subset of poor models can be seen. For example, Figure 2 shows twenty-one models with R^2 below 0.7.

Source: [Article Notebook](#)

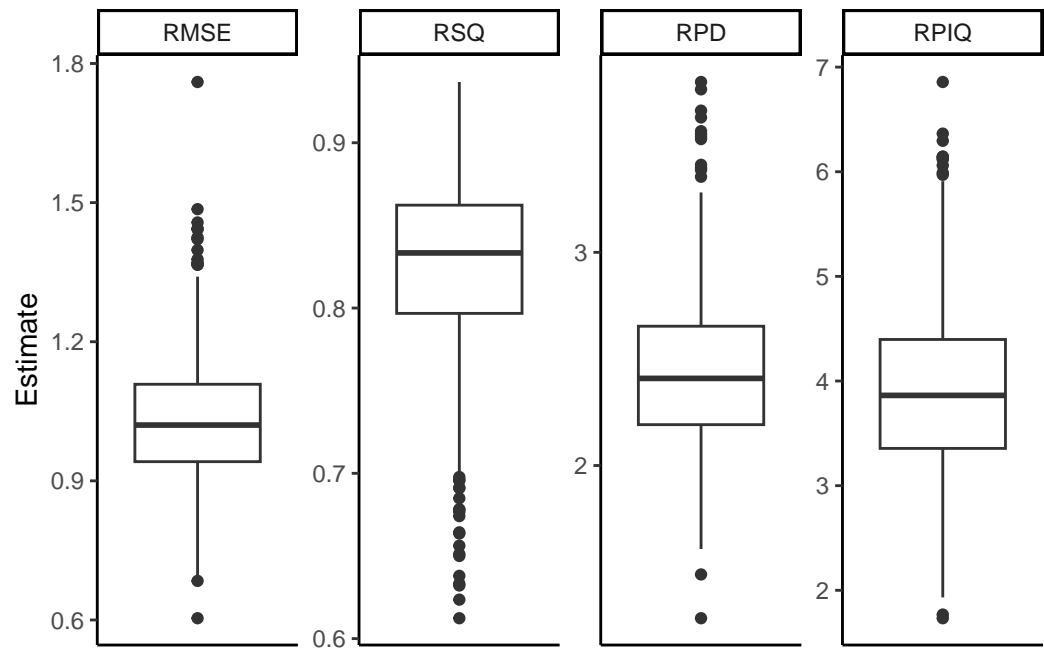


Figure 2: Final model test set performance (1000 iterations)

Source: [Article Notebook](#)

Source: [Article Notebook](#)

Source: [Article Notebook](#)

Source: [Article Notebook](#)

Source: [Article Notebook](#)

Source: [Article Notebook](#)

Finally, the pattern of test set errors was examined on a per-sample basis Figure 3 .

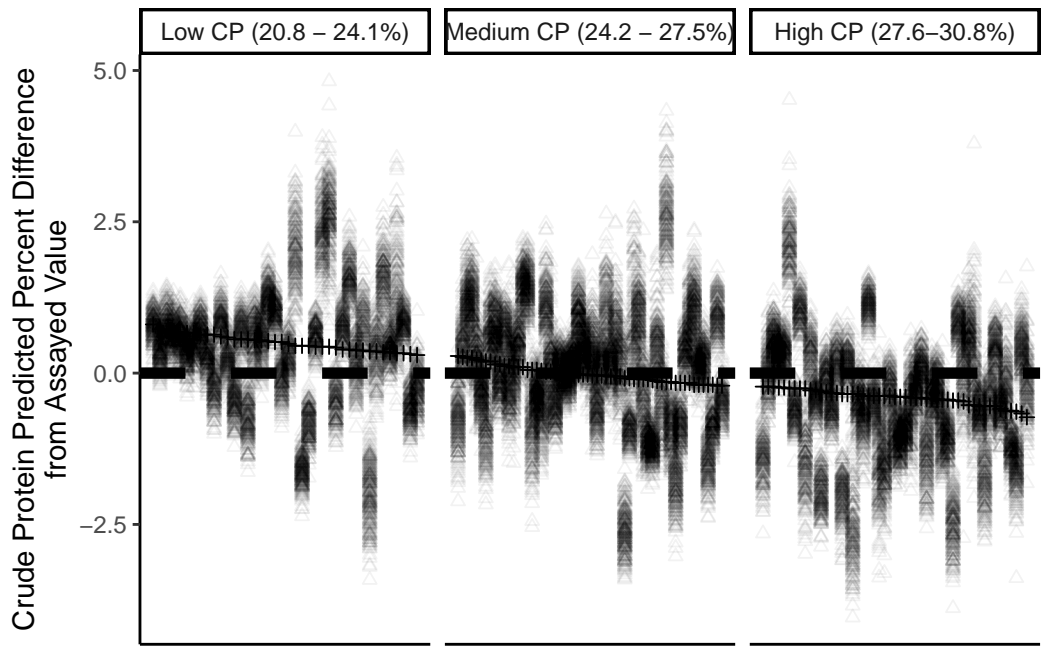


Figure 3: Test set prediction errors on a per-sample basis. Actual sample value set to 0, and samples ranked from least to greatest actual % CP value

Source: [Article Notebook](#)

Source: [Article Notebook](#)

To assess the patterns of errors within the models, a linear model was fit considering the mean estimated error for each sample considering all models where that sample was in the test set when compared to the sample’s actual value. The models overestimated %CP by approximately 0.5 % in the lowest tertile and underestimated %CP by -0.01 % and -0.41 % in the middle and highest tertile, respectively

Source: [Article Notebook](#)

This study is limited in that it represents the creation of one model based upon spectra collected from one machine. NIRS calibrations can be unique to a particular machine, even if the machines compared are of the same model (Reeves, 2012). As well, the calibration and validation sets are relatively small.

This research showed the promise of the use of NIRS in order to make predictions concerning %CP in hemp grain using PLS. Promising preprocessing methods were identified and a model was validated. Further research could refine a CP model by including more samples, identifying promising spectral regions, or by examining other predictive methods.

0.4 ACKNOWLEDGMENTS

0.5 SUPPLEMENTAL MATERIAL

Table 3: Tally of hemp cultivars and locations. Private cultivars are labeled “cultivar1”, “cultivar2”, etc.

cultivar2	chazy	freeville	geneva	ithaca	willsboro	Total
altair				1		1
anka		1	3	5	2	11
bialobrzeskie		1	3	4	1	9
canda		1	1	1		3
cfx-1		1	2	5		8
cfx-2		1	2	4		7
crs-1	1	1	2	5		9
cultivar1		1				1
cultivar2				1		1
cultivar3				1		1
cultivar4				1		1
earlina 8			1			1
experimental1				1		1
experimental2				1		1
felina 32		1	2	3		6
futura 75		1	3	4		8
grandi		3	3	4		10
h-51			1	2		3
han-fn-h				1		1
han-nw				1		1
helenia		1				1
henola				2		2
hlesia				3		3
hliana			1	1		2
joey		1	1	1		3
katani		2	3	4		9
nebraska (feral)	1			1		2
pewter river		1				1
picolo		1	2	5		8
portugal			1			1
rocky hemp			1			1
sterling gold			1			1
swift	1	1		1		3
tygra		1	3	4		8
uso-31	2	1	2	4		9
wojko		1	3	4		8
x-59		2		1		3
Total	5	24	41	76	3	149

239 Source: [Article Notebook](#)240 **0.6 OPTIONAL SECTIONS**241 **0.7 REFERENCES**242 **0.8 FIGURES AND TABLES**243 Source: [Article Notebook](#)

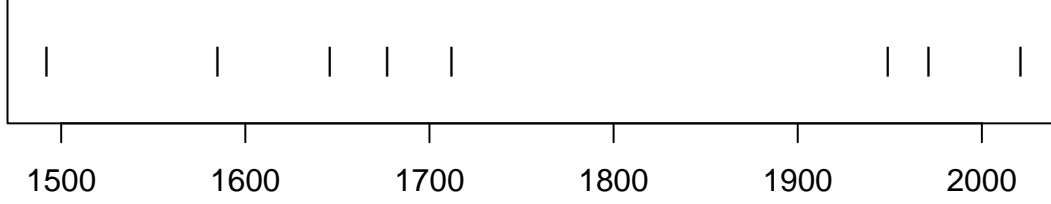


Figure 4: Timeline of recent earthquakes on La Palma

Source: [Article Notebook](#)

Source: [Article Notebook](#)

Based on data up to and including 1971, eruptions on La Palma happen every 79.8 years on average.

Studies of the magma systems feeding the volcano, such as ([marrero2019?](#)), have proposed that there are two main magma reservoirs feeding the Cumbre Vieja volcano; one in the mantle (30-40km depth) which charges and in turn feeds a shallower crustal reservoir (10-20km depth).

Eight eruptions have been recorded since the late 1400s (Figure 4).

Data and methods are discussed in Section 0.9.

Let x denote the number of eruptions in a year. Then, x can be modeled by a Poisson distribution

$$p(x) = \frac{e^{-\lambda} \lambda^x}{x!} \quad (1)$$

where λ is the rate of eruptions per year. Using Equation 1, the probability of an eruption in the next t years can be calculated.

Table 4: Recent historic eruptions on La Palma

Name	Year
Current	2021
Teneguía	1971
Nambroque	1949
El Charco	1712
Volcán San Antonio	1677
Volcán San Martin	1646
Tajuya near El Paso	1585
Montaña Quemada	1492

Table 4 summarises the eruptions recorded since the colonization of the islands by Europeans in the late 1400s.

La Palma is one of the west most islands in the Volcanic Archipelago of the Canary Islands (Figure 5).

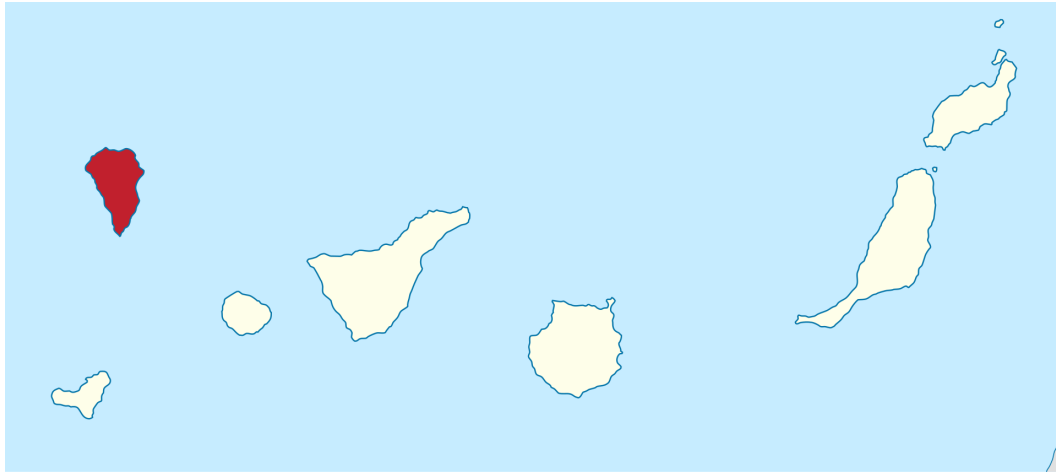


Figure 5: Map of La Palma

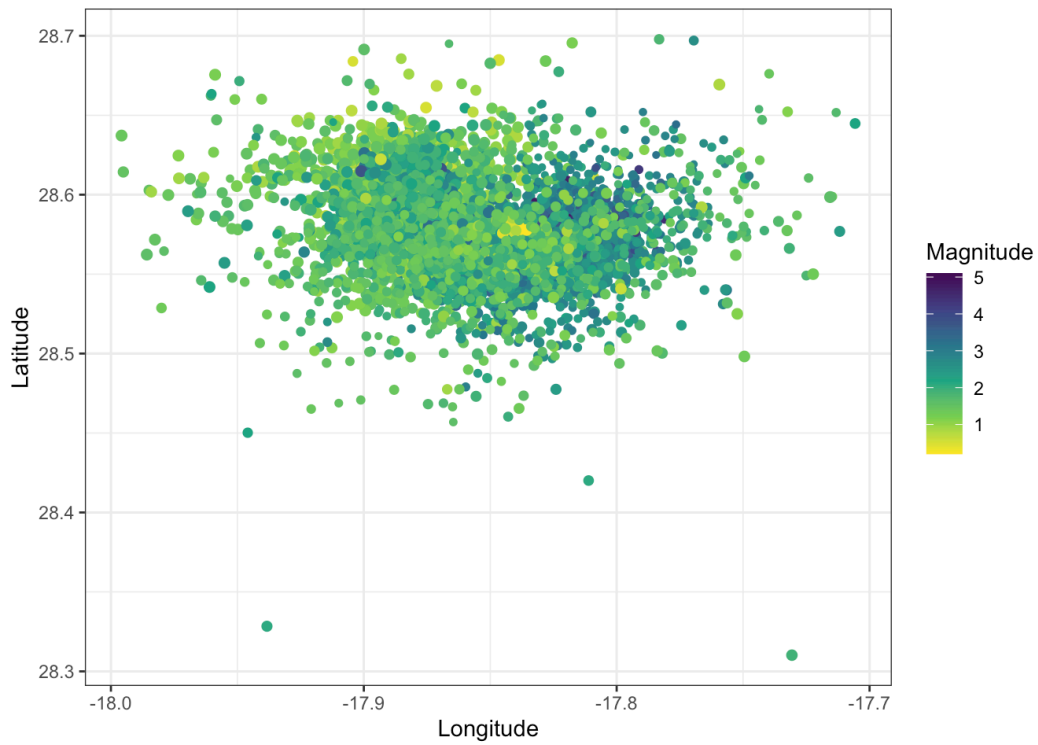


Figure 6: Locations of earthquakes on La Palma since 2017

262 Source: [Explore Earthquakes](#)

263 Figure 6 shows the location of recent Earthquakes on La Palma.

0.9 Data & Methods

0.10 Conclusion

References

- Barnes, R. J., Dhanoa, M. S., & Lister, S. J. (1989). Standard Normal Variate Transformation and De-Trending of Near-Infrared Diffuse Reflectance Spectra. *Applied Spectroscopy*, 43(5), 772–777. <https://doi.org/10.1366/0003702894202201>
- Barrett, T., Dowle, M., Srinivasan, A., Gorecki, J., Chirico, M., & Hocking, T. (2024). *data.table: Extension of “data.frame”*. <https://CRAN.R-project.org/package=data.table>
- Bárta, J., Roudnický, P., Jarošová, M., Zdráhal, Z., Stupková, A., Bártová, V., Krejčová, Z., Kyselka, J., Filip, V., Říha, V., Lorenc, F., Bedrníček, J., & Smetana, P. (2024). Proteomic Profiles of Whole Seeds, Hulls, and Dehulled Seeds of Two Industrial Hemp (*Cannabis sativa* L.) Cultivars. *Plants*, 13(1), 111. <https://doi.org/10.3390/plants13010111>
- Bellon-Maurel, V., Fernandez-Ahumada, E., Palagos, B., Roger, J.-M., & McBratney, A. (2010). Critical review of chemometric indicators commonly used for assessing the quality of the prediction of soil attributes by NIR spectroscopy. *TrAC Trends in Analytical Chemistry*, 29(9), 1073–1081. <https://doi.org/10.1016/j.trac.2010.05.006>
- Callaway, J. C. (2004). Hempseed as a nutritional resource: An overview. *Euphytica*, 140(1), 65–72. <https://doi.org/10.1007/s10681-004-4811-6>
- Chadalavada, K., Anbazhagan, K., Ndour, A., Choudhary, S., Palmer, W., Flynn, J. R., Mallayee, S., Pothu, S., Prasad, K. V. S. V., Varijakshapanikar, P., Jones, C. S., & Kholová, J. (2022). NIR Instruments and Prediction Methods for Rapid Access to Grain Protein Content in Multiple Cereals. *Sensors (Basel, Switzerland)*, 22(10). <https://doi.org/10.3390/s22103710>
- Ely, K., & Fike, J. (2022). Industrial Hemp and Hemp Byproducts as Sustainable Feedstuffs in Livestock Diets. In D. C. Agrawal, R. Kumar, & M. Dhanasekaran (Eds.), *Cannabis/Hemp for Sustainable Agriculture and Materials* (pp. 145–162). Springer. https://doi.org/10.1007/978-981-16-8778-5_6
- Garrido-Varo, A., Garcia-Olmo, J., & Fearn, T. (2019). A note on Mahalanobis and related distance measures in WinISI and The Unscrambler. *Journal of Near Infrared Spectroscopy*, 27(4), 253–258. <https://doi.org/10.1177/0967033519848296>
- Geyer, M., Mohler, V., & Hartl, L. (2022). Genetics of the Inverse Relationship between Grain Yield and Grain Protein Content in Common Wheat. *Plants*, 11(16), 2146. <https://doi.org/10.3390/plants11162146>
- Giancaspro, A., Giove, S. L., Blanco, A., & Gadaleta, A. (2019). Genetic Variation for Protein Content and Yield-Related Traits in a Durum Population Derived From an Inter-Specific Cross Between Hexaploid and Tetraploid Wheat Cultivars. *Frontiers in Plant Science*, 10. <https://doi.org/10.3389/fpls.2019.01509>
- Hayes, M. (2020). Measuring Protein Content in Food: An Overview of Methods. *Foods*, 9(10), 1340. <https://doi.org/10.3390/foods9101340>
- Kuhn, M., & Wickham, H. (2020). *Tidymodels: A collection of packages for modeling and machine learning using tidyverse principles*. <https://www.tidymodels.org>
- Kuhn, & Max. (2008). Building predictive models in r using the caret package. *Journal of Statistical Software*, 28(5), 1–26. <https://doi.org/10.18637/jss.v028.i05>
- Lenth, R. V. (2024). *emmeans: Estimated marginal means, aka least-squares means*. <https://CRAN.R-project.org/package=emmeans>
- Li, Y., Huang, Y., Xia, J., Xiong, Y., & Min, S. (2020). Quantitative analysis of honey adulteration by spectrum analysis combined with several high-level data fusion strategies. *Vibrational Spectroscopy*, 108, 103060. <https://doi.org/10.1016/j.vibspec.2020.103060>

- Liland, K. H., Mevik, B.-H., & Wehrens, R. (2023). *pls: Partial least squares and principal component regression*. <https://CRAN.R-project.org/package=pls>
- Luce, M. S., Ziadi, N., Gagnon, B., & Lévesque, V. (2017). Prediction of total carbon, total nitrogen, and pH of organic materials using visible near-infrared reflectance spectroscopy. *Canadian Journal of Soil Science*, 98(1), 175–179. <https://doi.org/10.1139/cjss-2017-0109>
- Luo, J., Ying, K., He, P., & Bai, J. (2005). Properties of Savitzky–Golay digital differentiators. *Digital Signal Processing*, 15(2), 122–136. <https://doi.org/10.1016/j.dsp.2004.09.008>
- Pinheiro, J. C., & Bates, D. M. (2000). *Mixed-effects models in s and s-PLUS*. Springer. <https://doi.org/10.1007/b98882>
- Pinheiro, J., Bates, D., & R Core Team. (2023). *nlme: Linear and nonlinear mixed effects models*. <https://CRAN.R-project.org/package=nlme>
- R Core Team. (2024). *R: A language and environment for statistical computing*. R Foundation for Statistical Computing. <https://www.R-project.org/>
- Rawal, A., Hartemink, A., Zhang, Y., Wang, Y., Lankau, R. A., & Ruark, M. D. (2024). Visible and near-infrared spectroscopy predicted leaf nitrogen contents of potato varieties under different growth and management conditions. *Precision Agriculture*, 25(2), 751–770. <https://doi.org/10.1007/s11119-023-10091-z>
- Reeves, J. B. (2012). Potential of Near- and Mid-infrared Spectroscopy in Biofuel Production. *Communications in Soil Science and Plant Analysis*, 43(1-2), 478–495. <https://doi.org/10.1080/00103624.2012.641844>
- Rinnan, Å., Berg, F. van den, & Engelsen, S. B. (2009). Review of the most common pre-processing techniques for near-infrared spectra. *TrAC Trends in Analytical Chemistry*, 28(10), 1201–1222. <https://doi.org/10.1016/j.trac.2009.07.007>
- Roberts, C. A., Workman, J., & Reeves, J. B. (2004). *Near-infrared spectroscopy in agriculture*. American Society of Agronomy.
- Stevens, A., & Ramirez-Lopez, L. (2024). *An introduction to the prospectr package*.
- Waring, E., Quinn, M., McNamara, A., Arino de la Rubia, E., Zhu, H., & Ellis, S. (2022). *skimr: Compact and flexible summaries of data*. <https://CRAN.R-project.org/package=skimr>
- Wickham, H., Averick, M., Bryan, J., Chang, W., McGowan, L. D., François, R., Grolemond, G., Hayes, A., Henry, L., Hester, J., Kuhn, M., Pedersen, T. L., Miller, E., Bache, S. M., Müller, K., Ooms, J., Robinson, D., Seidel, D. P., Spinu, V., ... Yutani, H. (2019). Welcome to the tidyverse. *Journal of Open Source Software*, 4(43), 1686. <https://doi.org/10.21105/joss.01686>
- Williams, P. C. (1975). Application of near infrared reflectance spectroscopy to analysis of cereal grains and oilseeds. *Cereal Chemistry*, 52(4 p.561-576), 576–561.
- Wold, S., Sjöström, M., & Eriksson, L. (2001). PLS-regression: A basic tool of chemometrics. *Chemometrics and Intelligent Laboratory Systems*, 58(2), 109–130. [https://doi.org/10.1016/S0169-7439\(01\)00155-1](https://doi.org/10.1016/S0169-7439(01)00155-1)